Impact of Uncommanded Effector Motions on Shuttle Consumables

M. S. Evanbar,* D. J. Simkin† and G. G. Altman‡
Rockwell International, Downey, California

Uncommanded thrust vectoring and aerosurface motions have concerned Space Shuttle designers, engineers, and flight planners since these motions were first discovered during early testing and flight simulation. These motions use hydraulic power and consume additional fuel. Clearly, uncommanded motion of these controls during Shuttle ascent, entry, and descent represents a potential impact to consumables margins and to payload weight. This article defines the two basic sources of uncommanded activity as hardware and flight control-related sources. The impact of these sources of uncommanded activity on consumables was successfully modeled by the authors. The model was also employed to allocate consumables reserves. The intent of the authors is to share with the reader the observed incidences of uncommanded activity, the formulation of the model, its application, and the reconciliation of model results with actual flight data.

Introduction

UNCOMMANDED effector motion is important to the control system designer, the power hydraulics subsystem designer, the consumables analyst, and the mission planner. Space Shuttle effectors under consideration include: inboard and outboard elevons, rudder, speed brake, body flap, and the main engine thrust vector control. These units control the motion of the vehicle during aerodynamic flight so that only the ascent and entry phases of a mission are germane to this discussion. Idealized use of energy comes from providing actuator motion to control the vehicle (aerodynamic force encountered in flight). There are also nonideal uses of energy that require the effectors to consume energy beyond their idealized thermodynamic requirements. The first group of nonidealities, familiar to the consumables analyst, consists of mission and subsystem performance uncertainties which deviate from ideal performance. These include pump characteristic uncertainties, specific fuel consumption uncertainties, turbulence, use of automatic vs control stick control steering, and timeline deviations. The second type of nonideality consists of noncommanded effector vibrations such as flight control limit cycling and power drive unit dither. These vibrations consume energy and, therefore, propellant. The motions can be very complex. They have been analyzed only recently for Shuttle systems and are the major topic of this paper.

Uncommanded effector motion could cause excess propellant consumption and violate planned mission margins. It is important, therefore, that these motions be understood and accounted for in mission planning and postflight data analysis.

To understand these motions, one must understand Shuttle subsystems and missions. The important related subsystems involved are the auxillary power unit (APU) (Fig. 1) and the hydraulic subsystem (Fig. 2).

Presented as Paper 82-1605 at the AIAA Guidance and Control Conference, San Diego, Calif., Aug. 9-11, 1982; received Aug. 23, 1982; revision received April 16, 1984. Copyright © American Institution of Aeronautics and Astronautics, Inc., 1982. All rights reserved.

*Operations Manager, Shuttle Orbiter Division.
†Project Manager, Shuttle Orbiter Division.
‡Technical Specialist, Shuttle Orbiter Division.

Background

APU Subsystem

Hydraulic power is generated by pumps which are driven by the APU and which operate during the ascent and entry/landing phases. Each of three APU's performs specific hydraulic functions, which are shared in case of a system failure. Each provides up to 135 hydraulic horsepower (hp) for a total of 405 hp. Each APU subsystem (Fig. 1) consists of a fuel tank, fuel distribution and servicing system, APU and controller, cooling system fuel pump and fuel control valve, and a thermal control system.

The APU gear-driven fuel pump supplies fuel to a catalyst bed gas generator; the generator's exhaust drives a turbine which, in turn, drives the hydraulic pump through a speed reduction gearbox. The gearbox lubrication oil is circulated through the hydraulic subsystem spray water boiler (SWB) for cooling.

Hydraulic Subsystem

Aerodynamic flight control is provided to the elevons by linear servoactuators controlled by four electrohydraulic servovalves (4-channel) integral with the actuator. The speed brake function is provided by a split rudder. Mechanical rotary actuators are driven by servocontrolled hydraulic motors to provide both rudder and speed brake control.

Main engine thrust vectoring is controlled by linear balanced-piston servoactuators, one for the pitch axis and one for the yaw axis for each of the three main engines. The servoactuator is controlled by four electrohydraulic servo valves (4-channel) integral with the actuator.

Main landing gear, noselanding gear, and the umbilical retractor are shown in Fig. 1 for completeness, but are not involved in the uncommanded motions under consideration.

Mission Description

Figure 3 summarizes the flight phases for a typical mission and for contingency missions. Return to launch site (RTLS) is shown as a dashed line, as are abort once around (AOA) and the transatlantic (TAL) site aborts. The APU and associated hydraulic functions required during flight phases are shown in the functions table of Fig. 3. It may be observed that some of the effectors are used only during ascent; thus their power drains are avoided for the remainder of the mission by isolating their hydraulics from the operating system after orbit is achieved. The thrust vector control, engine control, and external tank umbilical effectors are in this category.[1-3]

Flight Simulation Laboratory

Before actual flight, predictions of effector duty cycles and consumables must include flight variables such as wind, turbulence, manual vs automatic control, aerodynamic coefficients, and system contingencies/failures.

Predictions of effector/APU duty cycles must be made before actual flight to determine adequacy of consumables for the envelope of flight conditions which were reasonably possible for Shuttle flight. For the predictions to be made, hundreds of runs were conducted in the Flight Simulation Laboratory (FSL). FSL studies how the Orbiter flies with the crew at the controls by simulating vehicle and system dynamics as well as flight environments under real-time conditions.[4].

Since it was designed to operate independently or in conjunction with other laboratories, the FSL contains two distinct hybrid computer systems and interface equipment. One of the systems solves math models of vehicle characteristics and operates with the Orbiter on-board avionics and software systems. The other hybrid system simulates an environment to verify the developmental systems, which are made to "think" they are operating in actual flight situations.

During descent-to-landing simulation, the flight crew uses the instrumentation and data displayed in the mockup to monitor the flight or to take manual control of the elevons and other movable aerodynmic surfaces and bring the vehicle to a runway landing. The variables introduced by the computers and the data associated with the Orbiter's controllability during the test are used to evaluate critical flight parameters for the landing sequence.

Sources of Uncommanded Effector Activity

Uncommanded aerosurface activity has been observed during vehicle 1) level approach and landing testing (ALT) mated flight, 2) hot fire tests, 3) the Aug. 1980 closed-loop dynamic stability test, and 4) in the FSL.

Uncommanded effector activity has two basic sources: 1) it can be hardware related, such as stickfriction and/or gear-train backlash inducing system instability, or 2) it can stem from flight control characteristics, such as signal noise. Frequently these two sources interact, leading to system oscillations that otherwise would be damped out. Dynamic loads also can induce cycling activity as a result of hysteresis and bending-body interactions.

Hardware-Induced Oscillation

The power drive unit (PDU) is a hydraulic servomotor that drives the body flap and speed brake during flight. Specific hardware-induced limit cycle in the PDU has been observed in development testing,[5] in OV-102, in the Flight Control Hydraulics Lab (FCHL), and in qualification PDU's. When oscillations were first observed during development testing, a study was conducted to characterize their natures and cause. The study resulted in the following observations.

1) As a result of the low damping and tendency of the PDU to overshoot a given positions, any external disturbance starts the PDU moving.

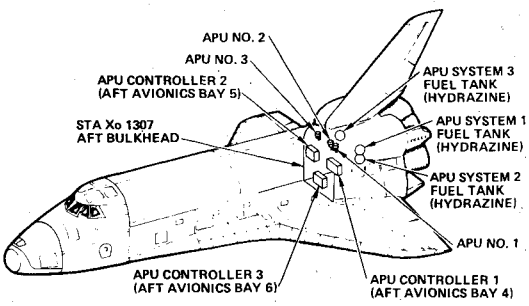

Fig. 1 Auxiliary power unit subsystem.

2) Once a motor breaks out, the pressure required to sustain motion is less than the starting pressure and the motor accelerates and overshoots the command.

3) The outer loop electronic sensing the motion provides a countering-feedback command.

4) The power valve moves in response to the command by decreasing flow to the motors.

5) However, because the speed-summing gearbox and power valve are out of synchronization, one of the motors accelerates rapidly in the opposite direction to the initial movement.

6) Because of system nonlinearities, the limit cycle continues.

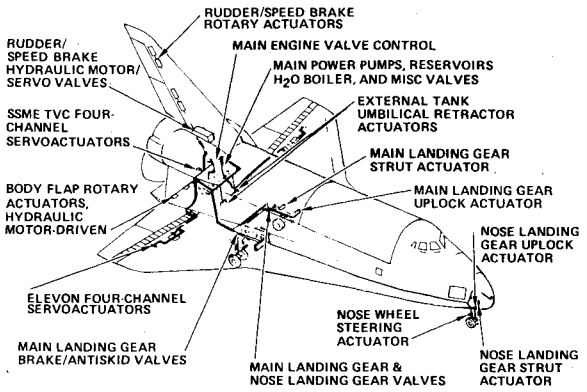

Fig. 2 Hydraulic subsystem.

Table 1 Observed incidents of PDU limit cycling

Effector	Amplitude, deg, peak to peak	Frequency, Hz	Rate, deg/sec	Comments
Rudder	0.190	1.00	0.76	T<50°F Qual unit worst-case observation
Rudder	0.065	0.47	0.12	Development unit
Rudder	0.055	0.52	0.11	Development unit
Rudder	0.065	1.17	0.30	Development unit
Rudder	0.040	0.60	0.10	Development unit
Rudder	0.045	0.52	0.09	Development unit
Rudder	0.065	0.84	0.22	Development unit
Rudder	0.065	0.58	0.15	Development unit
Rudder	0.055	0.63	0.14	Development unit
Rudder	0.055	0.98	0.22	Development unit
Rudder	0.060	1.15	0.28	Development unit
Rudder	0.090	1.36	0.49	Development unit
Speed brake	0.210	0.50	0.42	T>100°F Qual unit worst-case observation

Rate summary (deg/s)

Rudder	3-sigma high	=	0.56	Development unit
Rudder	Observed worst case	=	0.76	Qual unit
Speed brake	Observed worst case	=	0.42	Qual unit

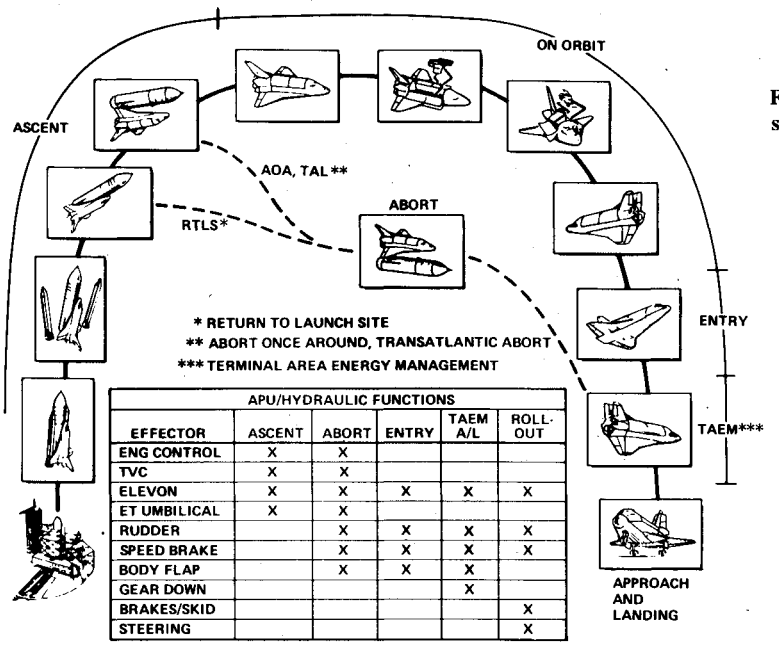

APU/HYDRAULIC FUNCTIONS					
EFFECTOR	ASCENT	ABORT	ENTRY	TAEM A/L	ROLL-OUT
ENG CONTROL	X	X			
TVC	X	X			
ELEVON	X	X	X	X	X
ET UMBILICAL	X	X			
RUDDER		X	X	X	X
SPEED BRAKE		X	X	X	X
BODY FLAP		X	X	X	
GEAR DOWN				X	
BRAKES/SKID					X
STEERING					X

Fig. 3 Space Shuttle mission description summary.

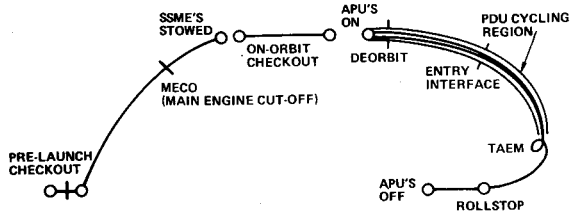

Fig. 4 Probable PDU limit-cycle regions in flight.

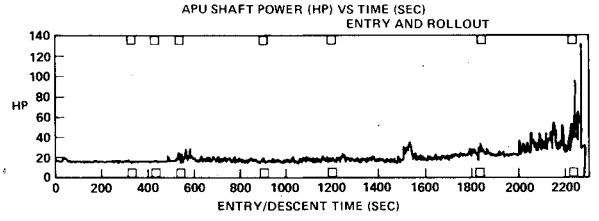

Fig. 5 Typical noise impacts on APU power requirements.

PDU limit-cycling incidence appears to be related to particular units, coupled with oil temperature. At unit start-up, the oscillation is characterized as 1 Hz in frequency with an amplitude of 45 deg of PDU shaft rotation. It occurs primarily in the rudder mode when the unit is started with cool oil. As the fluid heats past 110°F, the oscillaiton ceases. These characteristics vary from unit to unit.

Table 1 summarizes the known incidents and characteristics of this limit cycle. During the ascent mission phase, the speed brake is overdriven closed, precluding limit cycling during this period. Limit cycling of the PDU is most probable during entry and descent and when the surfaces are not slewing (Fig. 4).

System-Induced Oscillation

Limit cycling of the flight control system is uncommanded actuator activity originating from control system characteristics rather than hardware. This type of uncommanded aerosurface activity was observed during the August 1980 closed-loop dynamic stability test and in FSL/FCHL simulations. FCS limit cycling can stem from several sources: unfiltered general purpose computer (GPC) and rate gyro noise, bit toggling, etc, and dynamic load oscillations caused by hysteresis and bending-body interactions.

Some rigid-body noise, such as bit toggling and multiplexer-demultiplexer (MDM) noise, is passed to the APU controller despite the presence of filters in the flight control system and results in uncommanded effector motion. This type of activity is seen in FSL simulations and is modeled in the continuous system modeling program (CSMP) off-line simulations. It is characterized by "hash" in elevon position histories during entry, persisting from entry interface to landing (signals can be transmitted to the effectors only if the hydraulic system is pressurized). Figure 5 illustrates this noise impact on APU shaft power requirements, based on data from a FSL entry simulation. Commanded activity is visible as power peaks approximately 1,450 s from entry interface on this figure. Prior activity is uncommanded. This type of activity can be approximated by a sinusoidal signal.

Conditional stability oscillations caused by hardware/software interactions were observed during the Aug. 1980 closed-loop dynamic stability test (DST). Figure 6 illustrates such activity stimulated by roll gyro noise on elevon rate. Note the decay of the signal, which appears to have a periodicity of about 1.6 s, peak to peak.

The Orbiter is not a rigid body. The structure bends under load, and these deformations enter the control loop. Flex-body interactions of the control system occur when structural motion is sensed by the control system, which attempts to correct it, thus inducing oscillations of the control surfaces or gimbals. This type of effector activity is probable for thrust vector control of the Space Shuttle main engines and solid rocket boosters in ascent and on aerosurfaces in the latter phases of entry and descent. Often, first-, second-, and third-order components of this activity (harmonics) must be dealt with. The higher-order components of this additional duty cycle result primarily from hysteresis and body bending. The cumulative duty cycle is represented by the following:

$$\delta = \sum_{n=1}^{4} A_n \sin 2\pi f_n t \qquad (1)$$

where A_n = force effector deflection (deg) for each harmonic, f_n = frequency of steady-state signal (Hz), and t = period of cycling activity (s).

The values of A_n and F_n are design characteristics defined by testing, n represents the order component.

Simulation of Uncommanded Effector Activity

The impact of uncommanded effector activity on APU and SWB consumable usage is complex. The major variables include: 1) hydraulic system load requirements during the mission, 2) dispersed environment (primarily winds and turbulence), 3) aerodynamic variations, and 4) control stick steering (CSS) modes vs auto control.

Interpretation of data from nonitegrated analyses is difficult and misleading. One of the few viable approaches is simulation or modeling, based on man-in-the-loop test data or effector histories obtained off line from continuous system modeling. This technique makes use of the consumables model, which handles the uncommanded activity as additional power demand, superimposed on the commanded (ideal) demand. Figure 7 illustrates this simulation technique, starting with noise-induced duty cycle, which leads to additional hydraulic demand and a higher fuel rate and reduced margin for the mission.

Uncommanded-activity impacts on consumables are summed up for a mission by linking the uncommanded duty cycle for the mission phases and then modeling consumptions. The consumptions of the three systems, including load sharing and potential system failure impacts, may then be calculated.

The Simulation Data Base

Effector activity data are required before consumable usages can be assessed: these data are supplied by FSL (man in the loop) and continuous system modeling (off-line) simulations for entry and ascent, received as effector position histories. A varied sample of ascents and entries has been examined. Tables 2 and 3 illustrate some of the variables that form the study data base.

Dispersed environment impacts are implicit to the ascent and entry effector history data obtained from FSL and off-line models. The data contain rigid-body noise to varying degrees (signal noise not filtered out entirely by the FCS system). Aero variations and CSS mode impacts are also implicit in the data. Flex-body interactions and PDU limit cycling effects are not implicit, however, and must be superimposed on the simulations before they are imput to the consumables model for assessment.

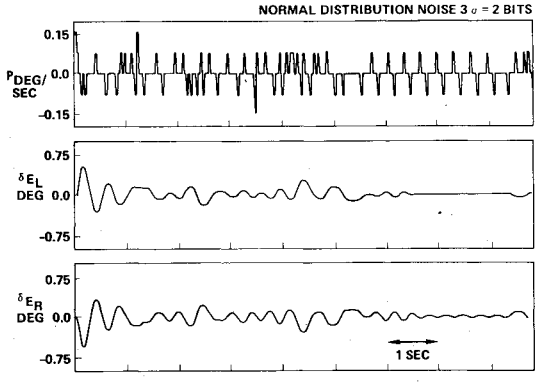

Fig. 6 Closed-loop response to gyro noise.

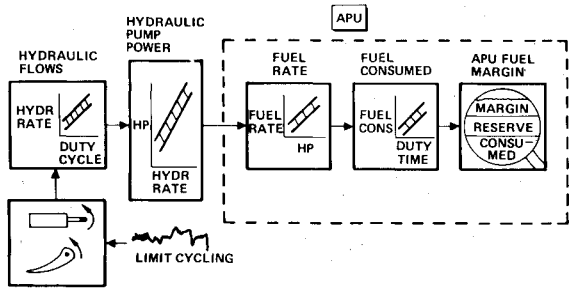

Fig. 7 Modeling noise as additional pump power demand.

Analysis Approach

An effective criterion for characterizing noise-related effector motion is required, particularly for noise sources not already present in available effector simulations; e.g., PDU limit cycling and flex-body interaction phenomena. The theoretical and uncommanded components of the cumulative travel of the effectors during ascent and entry, accumulated in

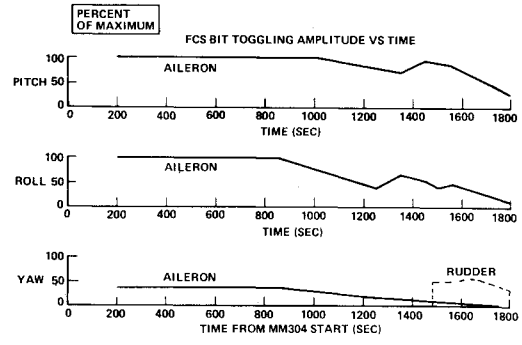

Fig. 8 Entry bit toggling schedule.

Table 2 Off-line (CSMP) ascent run matrix

Run description		Failures	
Stage	Winds	Type	Description
1	Mean vector wind	None	-
2	106.6-fps wind	None	-
1	50% wind	None	-
2	50% wind	AOA	SSME 3 at T = 266 s
1	95% wind	None	-
2	95% wind	ATO	SSME 2 at T = 460 s
1	50% wind	None	-
2	106.6-fps wind	None	-
1	95% wind	None	-
2	106.6-fps wind	None	-

106.6 fps steady-state wind

Table 3 FSL entry run matrix

Run description[a]			Failures	
Control	Turbulence	Steady wind	APU	RCS
Auto	No	None	None	None
Auto	Yes	None	None	None
CSS	No	None	None	None
CSS	Yes	None	None	None
Auto	Yes	East	None	None
Auto	Yes	West	None	None
Auto	No	None	No. 2,3	None
Auto	Yes	None	No. 2,3	None
CSS	Yes	None	No. 2,3	None
Auto	Yes	West	No.3	None
Auto	Yes	West	No.2,3	None
Auto	No	None	No.3	6 jets
CSS	No	None	No. 3	6 jets
Auto	No	N.E.	No.3	6 jets
Auto	Yes	N.E.	No.3	6 jets
CSS	Yes	N.E.	No.3	6 jets

[a] Real-time FSL simulation includes MDM noise.

Table 4 Comparison of filtered vs unfiltered FSL simulation for STS-1 entry

Statistical data for 8 STS-1 simulations	Average sim time, min	Duty cycles, deg					APU fuel usage, lb		
		Left	Right	Rudder Averages	Speed brake	Body flap	Sys 1	Sys 2	Sys 3
Unfiltered	38.174	2580	2426	459	1076	401	78.9	87.0	82.0
Filtered	38.174	1249	1181	276	566	121	72.8	74.4	71.9
Difference		1331	1245	183	510	280	6.1	12.6	10.1
				Standard deviation					
Unfiltered		508	442	148	279	129	3.2	3.5	3.1
Filtered		554	505	111	117	20	0.4	2.3	1.7
STS-1 actual		760	834	412	685	140	64.4	80.5	76.3

degrees of motion, serve this purpose. This criterion is also being used to assess the amount of rigid-body noise in simulations already containing noise by comparison with the theoretical duty cycles. Approach and landing (ALT) data contained considerable noise; application of successively stringent filtering removed more and more of the duty cycle from the flight data.

Based on the duty cycle criterion, a procedure was developed to characterize the noise-induced duty cycle contained in simulations or flight data such as observed in ALT. It consists of two steps: 1) "fingerprint" the noise-related duty cycle by summing degrees of travel during periods of known noncommands, such as during depressurized operation or during early entry; 2) model the noise-related rate component of the duty cycle for an oscillation of given frequency and amplitude during the oscillatory period.

When isolated and defined, this noise-related duty cycle then can be subtracted from data containing noise to obtain the theoretical duty cycle or it can be superimposed on noiseless duty cycle simulations (space vehicle dynamic simlator and Shuttle procedures simulator) to model noise impacts.

Noise sources not easily isolated and identified in flight data, such as PDU limit cycle and flex-body-induced cycling, can be superimposed on mission duty cycles if a reasonable amplitude and frequency scenario can be synthesized. Figure 8 is an example of such a schedule for entry bit toggling, modeled as an additional duty cycle. Once such a schedule is constructed, it is possible to calculate the consumable reserves for uncommanded activity during a mission and ensure that there are sufficient margins. The method of calculation is described in the following sections.

Modeling Techniques

Computation of Comsumables Budgets

During a textbook mission such as the first flight (STS-1), only a fraction of the available fuel and water is used; however, contingencies such as APU or hydraulic system failure, mission aborts, or a combination of these two, could cause fuel or water consumption to approach the available limit. In addition, fuel and water mission budgets must provide for system performance uncertainties, such as uncommanded motion of the effectors.

Rockwell International has written a computer program to calculate consumable usage, mission reserves, and operational margins. The program, called APEX, computes the mission usage, reserves, and margins from effector movement time histories, system characteristics, mission event time lines, and certain environmental factors, such as ambient air pressure, structural heat buildup, and spacecraft control modes (automatic control vs control-stick steering). The process of converting effector motion into consumables via the computer is depicted in Fig. 9. At a given point in time, effector motion (in angular rates) is translated into a hydraulic fluid flow rate. This flow is summed with other effector flow rates to result in a total flow rate (or pump load). This is then converted into hydraulic pump power, which is equal to the output (shaft) power of the APU driving this system.

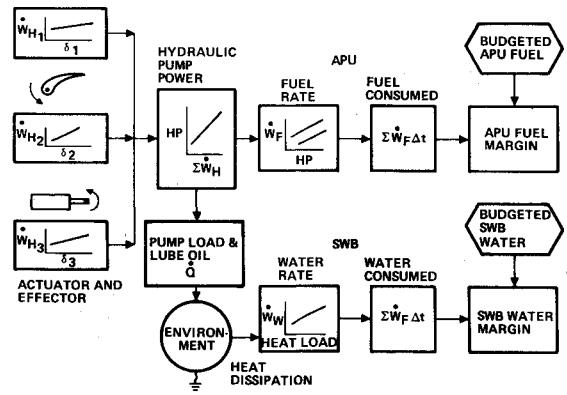

Fig. 9 Calculating fuel and cooling water usage.

The APU fuel consumption rate is nearly linearly related to APU shaft power. Integrating the fuel consumption rate over APU duty time yields theoretical fuel usage for the mission. Adding reserve amounts and comparing the result to the fuel available yields the mission margin for the APU/hydraulic system.

Cooling of the APU gearbox lubrication oil begins approximately 7 min after APU powerup. Heat from the hydraulic systems is first dissipated to the environment and the Orbiter structure. There is a delay of about 25 min until the hydraulic fluid (pump load) becomes hot enough to require cooling by way of the SWB. These effects are accounted for in the computation of the theoretical SWB water demand. Mission margins for SWB are calculated in a fashion similar to that of the APU fuel.

Modeling Consideration

Simulated effector motion time history imputs to the APEX program are derived from simulated angular deflection time histories at a sampling frequency of 25 Hz. These deflections are converted into angular deflection time rates at 0.5 Hz, the sampling frequency of the APEX program. The chain of events for calculating fuel and water usage is illustrated in Fig. 9.

Figure 10 illustrates this process. Actual deflection time histories are sampled at 25 Hz. From this sample of deflection vs time, deflection rates vs time are calculated. For the applied energy source, the direction of the deflection rates is immaterial. Therefore, negative rates are rectified and averaged over the low-frequency interval. In the example shown, which for clarity samples a 1 s period at 0.1-s intervals, the

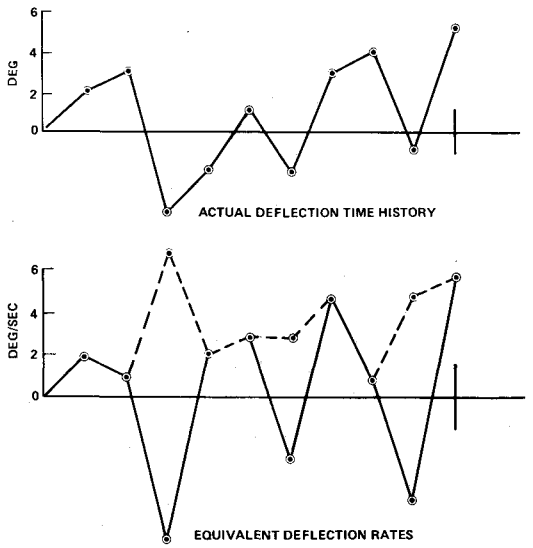

Fig. 10 Effector deflection histories.

equivalent rate is 3.5 deg/s instead of 0.5 deg/s, as it would be if negative rates were not rectified.

The principle is extended to the superposition of uncommanded motion upon the real signal. Assume that the amplitude and frequency of the uncommanded motion are known and that the wave form is sinusoidal.

Differentiating with respect to time to obtain incremental angular rate yields the following:

$$\dot{\delta} = 2\pi fA \cos 2\pi ft \tag{2}$$

$$= \omega A \cos \omega t \tag{3}$$

Averaging over a half-cycle (equal to π radians) yields the following:

$$\delta = \frac{2}{\pi} \cdot \omega A = 4fA \tag{4}$$

This is now the effective angular rate until either A or f is changed. The quantity in Eq. (2) is now superimposed over the existing unidirectional angular rate for the effector. Calculation of pump load, APU power, and fuel and water consumption proceeds as it would be without the perturbation.

Filtering Noise From Simulations

Effector deflection time histories from real-time entry simulations are likely to contain a certain amount of noise. This noise comprises unfiltered multiplexer-demultiplexer (MDM) signal noise not seen in flight data. STS-1 and STS-2 elevon and rudder duty cycle data indicate that this noise adds significant deflection to the simulated mission which results in a usage greater than predicted and a smaller flight planning margin. Two filtering techniques have been developed and used successfully to remove this noise. (These techniques are described in later paragraphs.) Filtering results based on these techniques are illustrated in Fig. 11. Waveform (a) is the raw FSL simulation data output; waveforms (b) and (c) are output following application of filtering methods 1 and 2, respectively. The cross marks on waveform (b) indicate reference readings, where successive readings indicate apparent "real" movement if filtering method 1 is used.

For illustration, Fig. 11 shows a noise rejection band considerably narrower in relation to the demonstrated waveform with actual FSL simulations. Computer runs have indicated that the filtered effector duty cycles (cumulative

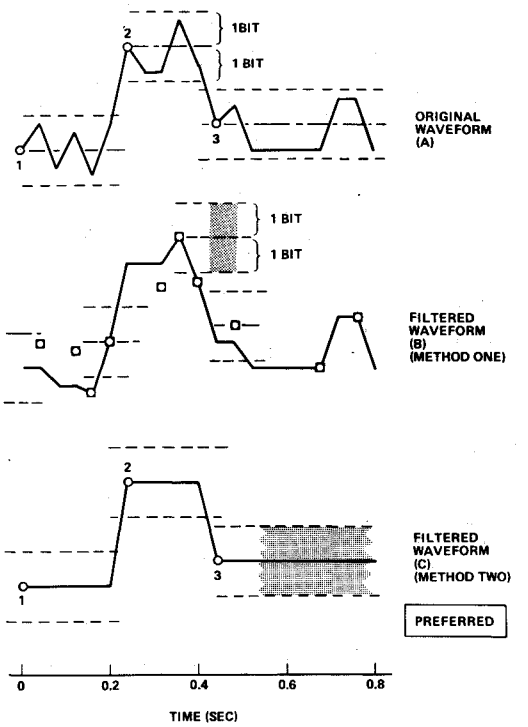

Fig. 11 Illustration of filtering FSL entry deflection histories.

angular deflections) ove a 38-min entry period are approximately equal for both filtering methods.

The two filtering techniques are based on output MDM bit granularity. Both methods start with an initial angular reading about which a noise dead band of plus/minus one bit is placed. Any apparent motion is said to be the result of MDM bit toggling.

The first technique measures the angular difference of successive MDM outputs. If the difference between the second and the first output is small enough to fall within the dead band, the actual angular difference is considered to be zero. This process is repeated for the third reading, with the second reading forming the preference for the noise dead band. This is true even if the second reading has been within the noise dead band about the first reading.

The second method differs from the first only in the treatment of the null differences between successive angular readings. A reference MDM output angular reading (which has established the dead band) remains unchanged until an MDM output is detected that exceeds the dead band. At that point, the dead band reference angle is updated, and the process is continued.

Eight STS-1 entry simulations were converted from the original 25-Hz data to equivalent 0.5-Hz aerosurface deflection rates. One run used no filtering; the other used filtering per method 2. The eight runs were chosen for their similarity with the actual STS-1 entry. Actual STS-1 entry aerosurface duty cycles are shown on the bottom of Table 4.

The averaged duty cycles over all eight simulations and the standard deviations are shown in Table 4. The APU fuel test usages shown are based on APU and hydraulic system characteristics updated since the STS-1 mission and are, therefore, not comparable with the actual STS-1 entry APU fuel usages. Based on the Table 4 data, two conclusions are reached.

1) The average values of the filtered duty cycles are acceptably close to the actual SST-1 entry duty cycles. Acceptability is defined as follows:

$$(\theta_S - \sigma_F) < \theta_F < (\theta_S + \sigma_F)$$

Table 5 Comparison of reconstructed consumables and flight data for STS-1

APU fuel usage (lb)		
System 1	System 2	System 3
	Actual	
122	162	160
	Reconstructed	
120	170	157
	Variation (%)	
+1.8	−4.4	+1.8

Entry total aerosurface displacement (deg)				
Right elevon	Left elevon	Rudder	Speed brake	Body flap
		Actual		
834	760	412	685	140
		Reconstructed		
1,181	1,249	276	566	121

where θ_S represents the actual STS-1 duty cycles, θ_F represents the FSL simulation duty cycles filtered average, and σ_F represents the standard deviation of θ_F.

2) Average APU fuel recovery as a result of noise filtering ranges from 6 lb for system 1 to 13 lb for system 2.

It should be noted that there is considerable variation in duty cycle values and delta usages between and within individual simulations. Also, there is only a weak correlation between duty cycle and usage decrements. This is the result of nonlinearities within the hydraulic system modeling.

Flight Data Review and Consumable Reconstruction

After each Space Shuttle flight, the APU fuel and cooling water remaining in the tanks and lines are drained and weighed. These off-load weights are relatively accurate; a reasonable off-load error is plus/minus 1 lb. Subtracting the off-load weights from the loaded fuel and water weights yields the flight usage actuals.

Reconstruction of Consumables

Usages of consumables are reconstructed by remodeling with actual as-flown operating precedures and power-up and power-down sequences. Any significant variations in usage between the reconstructed and the weighed actual must be attributed to one or more of the following: 2) modeling error, 2) performance dispersions, and/or 3) uncommanded effector motions.

Modeling error is assumed to be less than 3% of actual usage, based on hot-fire tests. Performance dispersions stem mainly from specific fuel consumption uncertainties and, to a lesser extent, from hydraulic pump efficiency uncertainties. These uncertainties are typically 5% or less of actual usage. It may be concluded that any reconstructed usage that lags actual by 8% or more could be evidence of uncommanded effector motion.

Total degrees of travel for the aerodynamic surfaces as recorded during flight, may also be compared with those from the reconstruction. The reconstructed variation from actual in total aerosurface movement provides more direct evidence of uncommanded motion than does fuel consumed. Table 5 compares actual fuel usage and aerosurface displacement data for the first Shuttle flight with reconstructed equivalents. No conclusive evidence of uncommanded motion is evident from Table 5, although rudder, speed brake, and body flap actuals do show moderate excesses.

More flight data are required to verify the impact of uncommanded effector motion on Shuttle consumables. It may be concluded, however, that uncommanded effector motion did not affect APU consumables significantly during the first Space Shuttle flight.

Conclusions

More flight data are required to verify the impact of uncommanded effector motion on Shuttle consumables. It may be concluded, however, that uncommanded effector motions did not affect APU consumables during the first Space Shuttle flight significantly. Data from subsequent flights corroborate the conclusion that uncommanded effector activity is not a significant consumer of APU fuel. Recognizing this, flight planners reduced the fuel reserve for uncommanded motions for the third flight to 32% of the original reserve. For the eighth and subsequent flights, flight planners now statistically combine reserves for power drive unit (PDU) and flight control system (FCS) limit cycling, recognizing the uncorrelated nature of these effector motions.

The release of APU fuel from performance uncertainty reserves has given flight planners the flexibility to off-load APU for the eighth and subsequence flights. The studies and evaluation techniques described herein have positively influenced the Space Shuttle program.

References

[1] Schleich, W. T., "The Space Shuttle Ascent Guidance and Control," AIAA Paper 82-1497, Aug. 1982.

[2] Nakano, M. M., "Space Shuttle On-Orbit Flight Control System," AIAA Paper 82-1576, Aug. 1982.

[3] Bayle, G. P., "Entry Flight Control Off-Nominal Design Consideration," AIAA Paper 82-1602, Aug. 1982.

[4] "Flight Simulation Laboratory Configuration Definition and Math Model," Rockwell International, Downey, Calif. SOD 79-0102, Feb. 1981.

[5] De Vlieger, M., "Failure Analysis and Corrective Action Report," Sundstrand Corp., Rockford, Ill. AB4046-010, Aug. 1979.